Available online at www.sciencedirect.com

ScienceDirect

Geochimica et Cosmochimica Acta 191 (2016) 47–57

Geochimica et Cosmochimica Acta

www.elsevier.com/locate/gca

Natural synthesis of bioactive greigite by solid–gas reactions

Kensuke Igarashi [a,1], Yasuhisa Yamamura [b], Tomohiko Kuwabara [a,*]

[a] Faculty of Life and Environmental Sciences, University of Tsukuba, Tsukuba, Ibaraki 305-8572, Japan
[b] Faculty of Pure and Applied Sciences, University of Tsukuba, Tsukuba, Ibaraki 305-8571, Japan

Received 22 August 2015; accepted in revised form 4 July 2016; available online 14 July 2016

Abstract

Greigite, a ferrimagnetic iron sulfide $Fe(II)Fe(III)_2S_4$, is thought to have played an essential role in chemical evolution leading to the origin of life. Greigite contains a [4Fe–4S] cluster-like structure and has been synthesized in the laboratory by liquid-state reactions. However, it is unclear how greigite can be synthesized in nature. Herein, we show that greigite is synthesized by the solid–gas reaction of Fe(III)-oxide-hydroxides and H_2S. We discovered that the hyperthermophilic hydrogenotrophic methanogen *Methanocaldococcus jannaschii* reduced elemental sulfur, and the resulting sulfide generated greigite from hematite. The time course and pH dependence of the reaction respectively indicated the involvement of amorphous FeS and H_2S as reaction intermediates. An abiotic solid–gas reaction of hematite and H_2S (g) under strictly anaerobic conditions was developed. The solid–gas reaction fully converted hematite to greigite/pyrite at 40–120 °C within 12 h and was unaffected by the bulk gas phase. Similar abiotic reactions occurred, but relatively slowly, with aqueous H_2S in acidulous liquids using hematite, magnetite, or amorphous FeO(OH) as starting materials, suggesting that greigite was extensively produced in the Hadean Eon as these Fe(III)-oxide-hydroxides were shown to be present or routinely produced during that era. Surprisingly, the obtained greigite induced methanogenesis and growth of hydrogenotrophic methanogens, suggesting that the external greigite crystals enhanced reactions that would otherwise require enzymes, such as [4Fe–4S] cluster-harboring membrane-bound hydrogenases. These data suggested that the greigite produced by the solid–gas and solid–dissolved gas reactions was bioactive.

Keywords: Amorphous iron sulfide; Cysteine desulfurase; Ferric oxide; Hydrogen sulfide; *Methanocaldococcus*

1. INTRODUCTION

Iron sulfides are thought to have played an essential role in chemical evolution (Wächtershäuser, 1992; Russell and Hall, 1997; Roldan et al., 2015). Among them, greigite ($Fe(II)Fe(III)_2S_4$) contains the cubic Fe_4S_4 unit (Rickard and Luther, 2007), similar to the [4Fe–4S] cluster that is crucial to life (Beinert et al., 1997). Fe–S clusters are biosynthesized by cysteine desulfurase (CDS) (Bandyopadhyay et al., 2008). However, numerous phylogenetic groups in the Euryarchaeota and Crenarchaeota phyla lack CDS genes (Liu et al., 2010). Thus, the origin of Fe–S clusters in the first life forms remains unknown. Although greigite is postulated as the origin of [4Fe–4S] clusters (Russell

Abbreviations: *CDS, cysteine desulfurase; FE-SEM, field-emission scanning electron microscopy; JCM, Japan Collection of Microorganisms; S^0, elemental sulfur; SRB, sulfate-reducing bacteria; XRD, X-ray diffraction*

* Corresponding author. Fax: +81 29 853 6614.
E-mail addresses: igarashi.kensuke@aist.go.jp (K. Igarashi), yasu@chem.tsukuba.ac.jp (Y. Yamamura), kuwabara@biol.tsukuba.ac.jp (T. Kuwabara).
[1] Present address: Bioproduction Research Institute, National Institute of Advanced Industrial Science and Technology (AIST), 2-17-2-1 Tsukisamu-Higashi, Toyohira-ku, Sapporo, Hokkaido 062-8517, Japan.

http://dx.doi.org/10.1016/j.gca.2016.07.005
0016-7037/

and Martin, 2004), there is no direct evidence to support this hypothesis. In addition to its biological importance, greigite is thought to be a promising material for the treatment of cancer hyperthermia (Chang et al., 2011; Paolella et al., 2011), the production of lithium-ion batteries (Apostolova et al., 2009), and applications as hydrogen storage devices (Cao et al., 2009) owing to its ferrimagnetic (Skinner et al., 1964), electrochemical (Skinner et al., 1964), and H_2-storage (Cao et al., 2009) properties, respectively.

Greigite can be synthesized in the laboratory by various methods (Berner, 1964; Wada, 1977; Dekkers and Schoonen, 1994; Chen et al., 2005; Cao et al., 2009; Paolella et al., 2011; Feng et al., 2013; Bauer et al., 2014). Among them, the polysulfide pathway, which involves mixing acidic Fe(II) and alkaline polysulfide solutions, is thought to represent the natural synthesis at alkaline hydrothermal vents (Russell and Hall, 1997). In this pathway, the initially formed amorphous FeS is converted to mackinawite (FeS), which is then converted, via the metastable intermediate greigite, to pyrite (FeS_2) (Berner, 1984; Hunger and Benning, 2007). In the conversion from mackinawite to greigite, Fe(II) is oxidized to Fe(III) under strictly anaerobic conditions in which polysulfides function as oxidizing agents (Berner, 1964; Rickard and Luther, 2007). This oxidation is thought to be the critical step in greigite synthesis. Interestingly, Fe(III)-oxide-hydroxides have not been tested as starting materials for greigite synthesis; they are expected to simply provide Fe(III).

Greigite is biologically synthesized extracellularly (Lefèvre et al., 2011) or intracellularly (Bertel et al., 2012) by sulfate-reducing bacteria (SRB). The product of sulfate reduction, sulfide, is crucial to the production of greigite. Sulfide is also produced by elemental sulfur (S^0)-reducing (hyper)thermophilic heterotrophs; however, these organisms are not thought to produce greigite (Igarashi and Kuwabara, 2014). The third known sulfide-producer is methanogens; some of these organisms have been reported to reduce S^0 and produce sulfide (Stetter and Gaag, 1983). However, since methanogenesis and sulfidogenesis are thought to compete for reducing equivalents, S^0-reducing ability is not considered useful for methanogenesis (Stetter and Gaag, 1983). Thus, whether methanogens produce greigite has not yet been studied to our knowledge. In the present study, we found that a hyperthermophilic hydrogenotrophic methanogen is a potent greigite-producer and developed an abiotic solid–gas reaction to synthesize bioactive greigite based on synthesis by the methanogen. Analogous solid–dissolved H_2S reactions likely reflect the natural synthesis of greigite because of its simplicity and versatility.

2. MATERIALS AND METHODS

2.1. Materials

Powdered S^0 (Wako, Osaka, Japan) was suspended in distilled water at 3 mol/L and sterilized by Tyndallization; namely, the suspension was autoclaved twice at 110 °C for 30 min with an interval of 24 h. Hematite (purity >97% [Wako] for growth medium; or purity = 99.9%, average particle size = 0.3 μm [Kojundo Chemical Laboratories, Sakado, Japan] for the solid–gas reaction), magnetite (purity = 99%, particle size ⩽1 μm; Kojundo Chemical Laboratories), and amorphous FeO(OH), prepared as described previously (Lovley and Phillips, 1986), were washed with and resuspended in distilled water at 0.6 mol/L, sterilized by autoclaving at 121 °C for 20 min, and stored under air at room temperature. Amorphous FeS, prepared as described previously (Brock and Od'ea, 1977), was washed with distilled water that had been bubbled with N_2 gas for 20 min, resuspended in the degassed distilled water at 0.6 mol/L, sterilized by autoclaving at 121 °C for 20 min, and stored at room temperature in an anaerobic workstation (Igarashi and Kuwabara, 2014) in which the gas phase was N_2:H_2:CO_2 (80:10:10).

2.2. Cultivation

The hyperthermophilic hydrogenotrophic methanogen *Methanocaldococcus jannaschii* JAL-1 (Jones et al., 1983) was obtained from the Japan Collection of Microorganisms (JCM) and maintained by successive cultivation in JCM 232 medium devoid of $NaHCO_3$ (Mc medium, pH 6.0) under a headspace of H_2:CO_2 (80:20) at 80 °C for 24 h. *M. jannaschii* was inoculated at 1×10^5 cells/mL into 12 mL Mc medium supplemented with 312 mmol/L S^0 and 30 mmol/L hematite (Mc + S^0 + hematite medium) in 68-mL serum bottles in the anaerobic workstation. After replacing the headspace with H_2:CO_2 (80:20), cultivation was performed at 80 °C for 32 h unless otherwise stated. The pH of the medium was lowered to 5.6 before cultivation due to the dissolution of CO_2.

The following methanogens were similarly cultured as specified. *Methanocaldococcus indicus* SL43 (L'Haridon et al., 2003) was cultured on H_2 in Mc medium under a headspace of H_2:CO_2 (80:20) at 80 °C and pH 5.6 for 32 h. *Methanothermobacter thermautotrophicus* ΔH (Zeikus and Wolee, 1972) was cultured on H_2 in JCM 231 medium devoid of Na_2CO_3 under a headspace of H_2:CO_2 (80:20) at 65 °C and pH 6.5 for 72 h. *Methanolobus tindarius* Tindari 3 (König and Stetter, 1982) was cultured on methanol in DSM 233 medium devoid of $NaHCO_3$ under a headspace of N_2 at 25 °C and pH 6.5 for 72 h.

2.3. Quantification of magnet-attracted substances

Cultures of *M. jannaschii* in Mc + S^0 + hematite medium were individually transferred to 15-mL disposable tubes, which were then capped after sealing with a piece of Teflon tape in the anaerobic workstation. The tubes were centrifuged at 1670*g* for 1 min. The supernatant was discarded, and the sediment was washed twice with the N_2-bubbled distilled water and once with 70% ethanol. The sediment was then vacuum-dried using a centrifugal concentrator (CC-105; TOMY, Tokyo, Japan) and dried overnight at room temperature in a desiccator under N_2. The dried sediment was ground with a mortar and pestle and weighed on a piece of powder paper. By applying a ferrite magnet purchased from a local market from underneath the powder paper, substances attracted by the magnet were

transferred onto another piece of powder paper and weighed. The magnet-attracted substances were quantified as the weight percent of the total sediment. Notably, non-magnetic substances bound to ferrimagnetic substances would be counted as magnet-attracted substances.

2.4. Solid–gas and solid–dissolved gas reactions

The 68-mL serum bottles were prepared in the anaerobic workstation, each accommodating 1 mL 1 M Na_2S (without adjustment of the pH) and a test tube ($\phi = 1$ cm, $L = 5$ cm) containing 0.63 mmol Fe in a dry mineral, either hematite (average particle size = 0.3 or 1.0 μm) or magnetite (particle size ⩽ 1 μm). The dry mineral was prepared by subjecting the precipitates from centrifugation of the autoclaved suspension to drying in a clean oven at 50 °C for up to 2 days. After sealing the serum bottle with a butyl rubber stopper (Nichiden-Rika Glass; Codes 309018) and an aluminum seal, the gas phase was replaced with Ar (purity = 99.999%), unless otherwise indicated, at ambient atmospheric pressure (1.0 atm). Gaseous H_2S (H_2S (g)) was generated in the serum bottles by injecting 0.55 mL 2 M H_2SO_4 into the 1 M Na_2S using a disposable Myjector syringe (TERUMO, Tokyo, Japan) (Fig. 1). The volume of H_2SO_4 was set so that the pH of the resulting solution became 5.6 ± 0.1 ($n = 3$), resembling the pH of *M. jannaschii* cultures. The serum bottles were incubated at 80 °C, unless otherwise stated, for the designated periods. This type of reaction was designated as the solid–gas reaction type. In similar solid–dissolved gas reactions, the iron sources were suspended in 1 M Na_2S, supplemented with H_2SO_4 as described above, and reacted with aqueous sulfides. The volume of 2 M H_2SO_4 was slightly different for some of the solid–dissolved gas reactions (e.g., 0.6 mL for amorphous FeO(OH) and 0.57 mL for amorphous FeS) to bring the pH of the solutions to 5.6. The products from amorphous FeO(OH) were washed with 0.5 N HCl and then washed six times with N_2-bubbled distilled water.

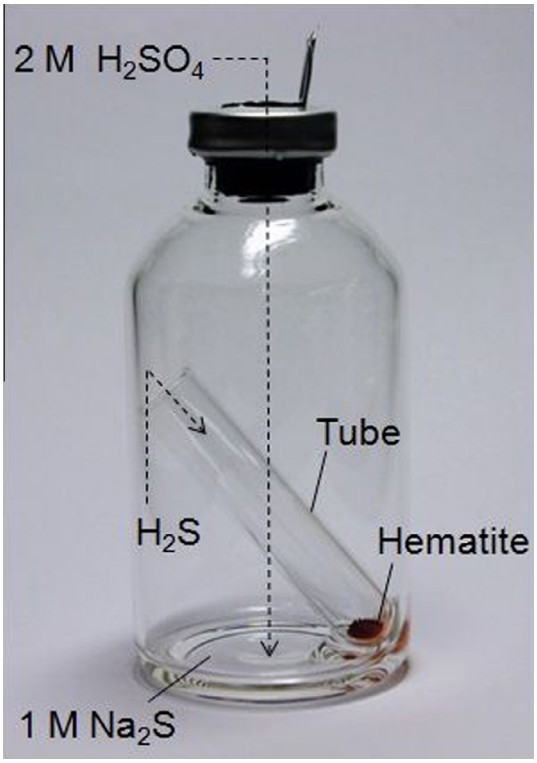

Fig. 1. The apparatus used for the solid–gas reaction.

2.5. X-ray diffraction analysis (XRD)

Culture sediments were collected by centrifugation at 1670*g* for 1 min. S^0 was mostly located within the lower part of the sediment. After discarding the supernatant, the upper part of the sediment was transferred using a spatula onto a silicon holder (Silicon Zero Background Sample Plate; SanyuShoko, Tokyo, Japan); this was expected to simplify the profile by eliminating the peaks derived from S^0. Homogenized sediments were also analyzed to determine whether any other minerals were formed. The holder was sealed with polyimide film (Nilaco Corporation, Tokyo, Japan) and vacuum grease to avoid desiccation and possible oxidation during the analysis. XRD profiles were obtained using an X-ray diffractometer (Ultima IV; Rigaku, Tokyo, Japan) for CuKα radiation scanning at a step interval of 0.02° 2θ and a counting time of 2 s with a 2θ range from 15° to 60°, operating at an accelerating voltage of 40 kV at 30 mA. Products of solid–gas and solid−dissolved gas reactions were analyzed as described above, except that the polyimide film and vacuum grease were not used with the products of solid–gas reactions; the polyimide film caused a broad peak at approximately 20°. All the products were analyzed on the day of preparation. Obtained profiles were compared with the Powder Diffraction File™ (ICDD, 2011) for identification of minerals.

2.6. Field-emission scanning electron microscopy (FE-SEM)

Culture sediments were placed onto SEM glass plates (diameter, 18 mm; Okenshoji, Tokyo, Japan), which had been coated with 0.1% (w/v) poly-L-lysine. After standing for 30 min at room temperature, the specimens were fixed with 2% (w/v) glutaraldehyde in 0.2 M sodium cacodylate (pH 7.2) for 2 h at room temperature and processed as described previously (Kuwabara and Igarashi, 2012). Products of solid–gas and solid−dissolved gas reactions were attached to carbon tape, which was placed on an aluminum stub. The specimens were observed using a field-emission scanning electron microscope (JSM-6330F; JEOL, Tokyo, Japan) as described previously (Igarashi and Kuwabara, 2014).

2.7. Other analytical methods

Cell density, methane, H_2, sulfide, and Fe(II) were determined from three independent serum bottles unless otherwise stated, and duplicate measurements were averaged for each culture. Densities of free cells in the liquid phase were determined by direct counting based on the autofluorescence from coenzyme F_{420} of the methanogen using an optical microscope (Eclipse E600;

Nikon, Tokyo, Japan) (Igarashi and Kuwabara, 2014) and bacteria counting chambers. Methane and H_2 in the gas phase were determined using gas chromatography (GC-8A; Shimadzu, Kyoto, Japan) with a Molecular Sieve 5A 60-80 column (2.0 m; Shinwa Chemical Industries, Ltd., Kyoto, Japan) (Igarashi and Kuwabara, 2014).

Fe(II) and sulfide in culture sediments were quantified as follows. Culture media were centrifuged to separate sediments and supernatants, as described previously (Igarashi and Kuwabara, 2014). The sediments were washed with and resuspended in 12 mL of N_2-bubbled water. During the homogenization of precipitates by swirling, 0.1-mL aliquots were transferred to 68-mL serum bottles in the anaerobic workstation. The serum bottles were capped with butyl rubber stoppers and aluminum seals, and the gas phases were replaced with N_2 (99.9999% pure). The samples were supplemented with 0.4 mL of 7.5 N HCl and each bottle was incubated at 100 °C in an oven for 20 min to dissolve the amorphous FeS and greigite (Cornwell and Morse, 1987). A 0.1-mL aliquot of each sample was taken using a Myjecter syringe (TERUMO, Tokyo, Japan), 0.02 mL of which was added to 1 ml of 0.1% 3-(2-pyridyl)-5,6-bis(4-phenylsulfonic acid)-1,2,4-triazine (ferrozine) in 50 mM *4-(2-hydroxyethyl)-1-piperazineethanesulfonic acid* (HEPES)-NaOH (pH 7.0) (Sørensen, 1982) to determine the Fe(II) content by the ferrozine method, using an ε_{562} of 27,900 M^{-1} cm^{-1} (Stookey, 1970). For sulfide determination, 10 mL of 1.2% $Zn(O_2CCH_3)_2(H_2O)_2$ (zinc acetate dihydrate) and 1.3 mL of 12% NaOH were added to the 0.4 mL of sample remaining in each serum bottle, which was then vigorously shaken to trap both gaseous and dissolved sulfides. Then, 2 mL of 0.1% *N,N,*-dimethyl-*p*-phenylenediamine in 5.5 N HCl and 1 mL of 0.046 M $FeCl_3$ in 1.2 N HCl were added (Chen and Mortenson, 1977) to determine sulfide by the methylene blue method using an ε_{664} of 95,000 M^{-1} cm^{-1} (Cenens and Schoonheydt, 1988). Fe(II) and sulfide in the culture supernatants were similarly determined by the ferrozine (Stookey, 1970; Sørensen, 1982) and the methylene blue (Chen and Mortenson, 1977; Cenens and Schoonheydt, 1988) methods, respectively.

3. RESULTS

3.1. Greigite synthesis by *M. jannaschii*

A previous study showed that hematite had the ability to recover methane production by fermenter (*Thermosipho globiformans*)-methanogen (*M. jannaschii*) syntrophy in the presence of S^0 (Igarashi and Kuwabara, 2014), suggesting that non-nutrient environmental minerals could enhance microbial activities. Because we are interested in the reduction of hematite mediated by S^0 reduction and the feedback from the resulting iron sulfides to the biological system, we attempted to evaluate the ability of the methanogen to reduce S^0.

M. jannaschii did reduce S^0 during growth at 80 °C, as evidenced by the production of aqueous sulfides (Fig. 2b). The reduction did not significantly affect methanogenesis or growth (Fig. 2a), contrary to the previously reported

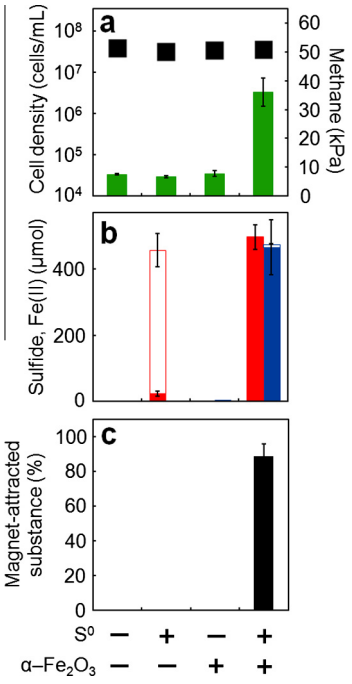

Fig. 2. Effects of S^0/hematite on *M. jannaschii*. *M. jannaschii* was cultured in Mc medium supplemented with nothing or S^0 and/or hematite for 32 h. (a) Cell density (closed squares) and methane production (green bars). (b) The amounts of sulfide (red bars) and Fe(II) (blue bars) from the sediment per serum bottle. The white bars indicate the corresponding components in the supernatant. (c) Fraction of magnet-attracted substances in the sediments. Error bars, mean ± SD ($n = 3$). The absence of error bars indicates that the bars are hidden by the symbols.

mesophilic and thermophilic S^0-reducing methanogens (Stetter and Gaag, 1983). Similarly, hematite alone had little or no effect on methanogenesis and growth, probably because it lacks cell permeability. Surprisingly, exposure to both of these substances almost quadrupled methanogenesis without affecting growth (Fig. 2a), suggesting the uncoupling of methanogenesis from ATP synthesis (Mountfort and Asher, 1979). During cultivation, the hematite turned black, suggesting its reduction to a possible iron sulfide by the methanogen-produced sulfide. This black product was not generated by the incubation of Mc + S^0 + hematite medium without the microorganism, and the amounts of sulfides solubilized from the sediments before and after the incubation were 0.19 ± 0.1 and 0.36 ± 0.1 μmol per serum bottle. The increase by the incubation (0.17 μmol/serum bottle) was far less than that by the cultivation (Fig. 2b), indicating little reduction of hematite without the microorganism. Interestingly, the black product was attracted by a magnet (Fig. 2c) but did not attract metal Fe. This ferrimagnetic product could be involved in the enhancement of methanogenesis.

Time courses of cultivation-dependent formation of ferrimagnetic product suggested that the iron sulfide initially formed at 12 h was nonmagnetic and then became ferrimagnetic after 16 h (Fig. S1a). These observations were supported by quantification of Fe(II) and sulfide, which were

solubilized in 6 N HCl in butyl rubber-stoppered serum bottles containing magnetically attracted substances (Fig. S1b–d). When the nonmagnetic, intermediate preparations produced after 12 h were quantitated for Fe(II) and sulfides, their 6 N HCl-solubilizable substances showed an Fe(II)-to-S ratio of 1.0 (mol/mol), while these preparations showed only peaks of hematite upon XRD (Fig. 3a), suggesting that the intermediate was undetectable by XRD and thus likely to contain amorphous FeS. Sediments from the 16-h to 32-h cultures showed decreasing hematite and increasing greigite peaks with time (Fig. 3b, c), whereas those from the 96-h culture exhibited peaks of greigite and pyrite but not hematite (Fig. 3d). These results suggested that hematite was first reduced to amorphous FeS, which was then converted to greigite and subsequently to pyrite, similar to the sequence in the polysulfide pathway (Hunger and Benning, 2007) except for the absence of mackinawite. Among these minerals, only greigite is ferrimagnetic; thus, we concluded that the ferrimagnetism originated from greigite.

FE-SEM of the sediments from the 32-h cultures showed nanoflakes, which are characteristic of greigite (Cao et al., 2009) (Fig. 3f), while those from the 96-h cultures showed framboidal pyrite-like botryoids (Butler and Rickard,

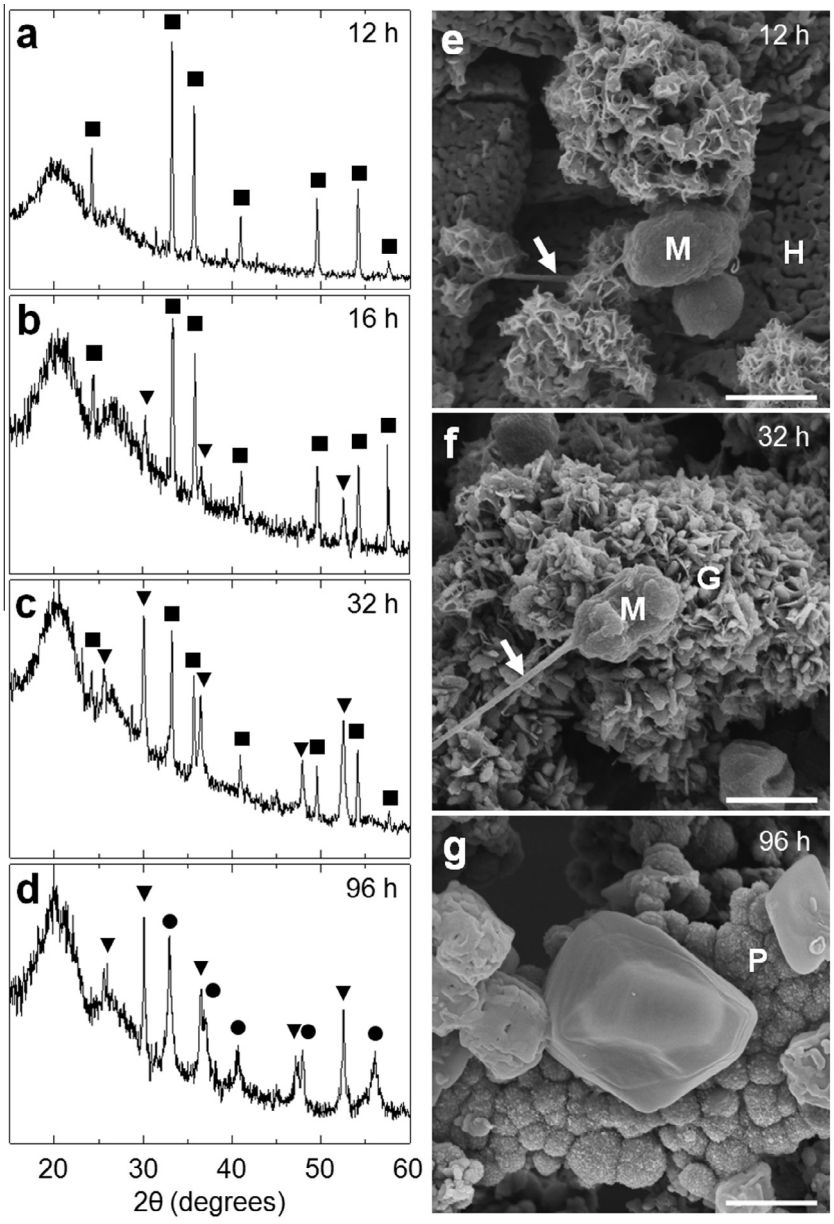

Fig. 3. Changes in minerals during cultivation. *M. jannaschii* was cultured in Mc + S^0 + hematite medium for the designated periods. The sediments were analyzed by XRD (a–d) and FE-SEM (e–g). Greigite, closed triangles. Hematite, closed squares. Pyrite, closed circles. The broad peak around $2\theta = 20°$ was derived from the polyimide film. The ordinate shows arbitrary signal intensity. A dividing *M. jannaschii* cell (M), as inferred from the cell shape, and an accompanying bridge (*arrow*) made from flagella (Igarashi and Kuwabara, 2014); hematite (H); greigite-like nanoflakes (G); and framboidal pyrite-like botryoids (P). Bars: 1 μm.

2000) and layered structures with smooth surfaces (Fig. 3g), which may have contained greigite; the nanoflakes were very rare in the 96-h sediments. None of these structures were observed in the sediments at 12 h; instead, complex petal-like structures were observed (Fig. 3e). Cells of *M. jannaschii* attached to hematite (Igarashi and Kuwabara, 2014), possible amorphous FeS (Fig. 3e), and the nanoflakes (Fig. 3f), suggesting that the sulfide emitted from the methanogen directly reduced the Fe(III) in the sediments.

The absence of greigite formation by S^0-reducing heterotrophs (Igarashi and Kuwabara, 2014) implied the inhibition by organics. Inclusion of nonproteinaceous organics (i.e., glucose, glycine, lactate, acetate, Casamino acids, or soluble starch) at 0.3% (w/v) in the medium did not interfere with greigite formation (Fig. S2). However, addition of tryptone or yeast extract apparently inhibited greigite formation in a concentration-dependent manner, although growth and methanogenesis were not apparently inhibited. Sufficient greigite to accelerate methanogenesis was probably formed even in the presence of proteinaceous organics, as described below. Inhibition of the formation of appreciable amounts of greigite by proteinaceous organics is consistent with the previously observed inability of (hyper) thermophilic heterotrophs to produce greigite.

3.2. Greigite synthesis by solid–gas and solid–dissolved gas reactions

The pH of the culture medium (5.6) suggested that the sulfide involved in greigite formation was H_2S (aq) based on the pH equilibrium profile of sulfides (Snoeyink and Jenkins, 1980). In fact, the pH dependence of cultivation-mediated greigite formation (Fig. S3) resembled the pH equilibrium profile. Based on this finding, we developed an abiotic solid–gas reaction of hematite and H_2S (g) to synthesize greigite, in which dry hematite in a test tube was reacted with H_2S (g) generated from 1 M Na_2S by the addition of 2 M H_2SO_4 in serum bottles (the solid–gas reaction; Fig. 1). The solid–gas reaction at 80 °C completely converted hematite to greigite and pyrite within 1 h (Fig. 4a). In contrast, when hematite was suspended in 1 M Na_2S followed by the addition of 2 M H_2SO_4 (the solid–dissolved gas reaction), only slight conversion occurred in the 1-h reactions (Fig. 4d), suggesting that reactions involving ionic sulfide species (HS^- and S^{2-}) were not responsible for the synthesis of greigite and pyrite. Prolonged solid–dissolved gas reactions for 3 h increased the amounts of greigite and pyrite, and decreased the amount of hematite (Fig. 4g), suggesting that essentially the same mechanism operated in the solid–gas and solid–dissolved gas reactions. The concentration of aqueous sulfides after the 1-h solid–gas reaction was 7.7 ± 0.8 mM, suggesting that the H_2S (g) concentration at the start of reaction is calculated to have been 15 mmol/L, about 2-fold that of aqueous sulfides. When hematite with an average particle size of 1 μm, instead of 0.3 μm, was used for the solid–gas reaction, the reactivity decreased significantly (Fig. S4e), suggesting that internal moieties in hematite grains did not react during the limited reaction time. Greigite and pyrite also formed from magnetite, with increased formation observed in the solid–gas reaction than in the solid–dissolved gas reaction (Fig. 4b, e). Prolonged solid–dissolved gas reactions with magnetite increased the amounts of greigite and pyrite (Fig. 4h). These characteristics are similar to those of hematite. The 1-h solid–gas reactions of hematite and magnetite produced 0.25 ± 0.04 and 0.20 ± 0.02 μmol H_2 per serum bottle, respectively. Unlike the polysulfide pathway (Hunger and Benning, 2007), mackinawite was not detected in these reactions, even after short reaction times (Fig. S4a–d).

Desiccation of amorphous FeS and amorphous FeO(OH) caused the formation of hardened large grains unsuitable for solid–gas reactions. When wet amorphous FeS was subjected to the solid–dissolved gas reactions, only mackinawite formed, even after 144 h (Fig. S4f). The absence of the expected conversion from mackinawite to greigite suggested that mackinawite was not a precursor for greigite. In contrast, the amorphous FeO(OH) turned black upon suspension in Na_2S and produced mackinawite and greigite in the 1-h solid–dissolved gas reaction (Fig. 4c). The difference in the reactivity between amorphous FeS and amorphous FeO(OH) suggested that inner moieties of amorphous FeO(OH) particles remained unreduced in 1 M Na_2S and thus were able to provide Fe(III) for greigite synthesis in the solid–dissolved gas reaction. The mackinawite would be produced by a bypass reaction from amorphous FeS (Fig. S4f) and was removed by washing the product with 0.5 N HCl (Lovley and Phillips, 1986) (Fig. 4f). Prolonged solid–dissolved gas reactions of amorphous FeO(OH) produced pyrite, apparently with maintenance of the relative levels of mackinawite and greigite (Fig. 4i), consistent with the conversion of greigite to pyrite and the de novo synthesis of greigite, as in the polysulfide pathway (Hunger and Benning, 2007). No products showed XRD peaks for S^0, a possible oxidation product from H_2S. Thus, S^0 may not be a product of the solid–gas and solid−dissolved gas reactions.

On FE-SEM, the products synthesized by the 1-h solid–gas reaction of hematite and magnetite showed flower-like structures encompassing microcavities (Fig. 4j) and spherical structures composed of variously sized grains with rugged surfaces (Fig. 4k), respectively. The products obtained by the 1-h solid–dissolved gas reaction of amorphous FeO(OH) followed by washing with 0.5 N HCl showed structures resembling an aggregate of 400 nm-long rods (Fig. 4l), which are in the range of nanobacteria (50 nm to 500 μm in length) (Kajander et al., 2003).

Although the solid–gas reactions produced H_2, the bulk gas phase of H_2 did not affect greigite synthesis (Fig. S5a). Similarly, N_2, CO_2, and CH_4 exhibited essentially no inhibition (Fig. S5c, e, f). As with ordinary chemical reactions, the higher the temperature, the faster the formation of greigite; for example, greigite synthesis was almost completed by 12 h at 40 °C and by 0.5 h at 120 °C (Fig. S5b, d).

3.3. Promotion of methanogenesis and growth of methanogens by greigite

To test the possible enhancement of methanogenesis by greigite, the products (0.63 mmol Fe) of solid–gas reactions

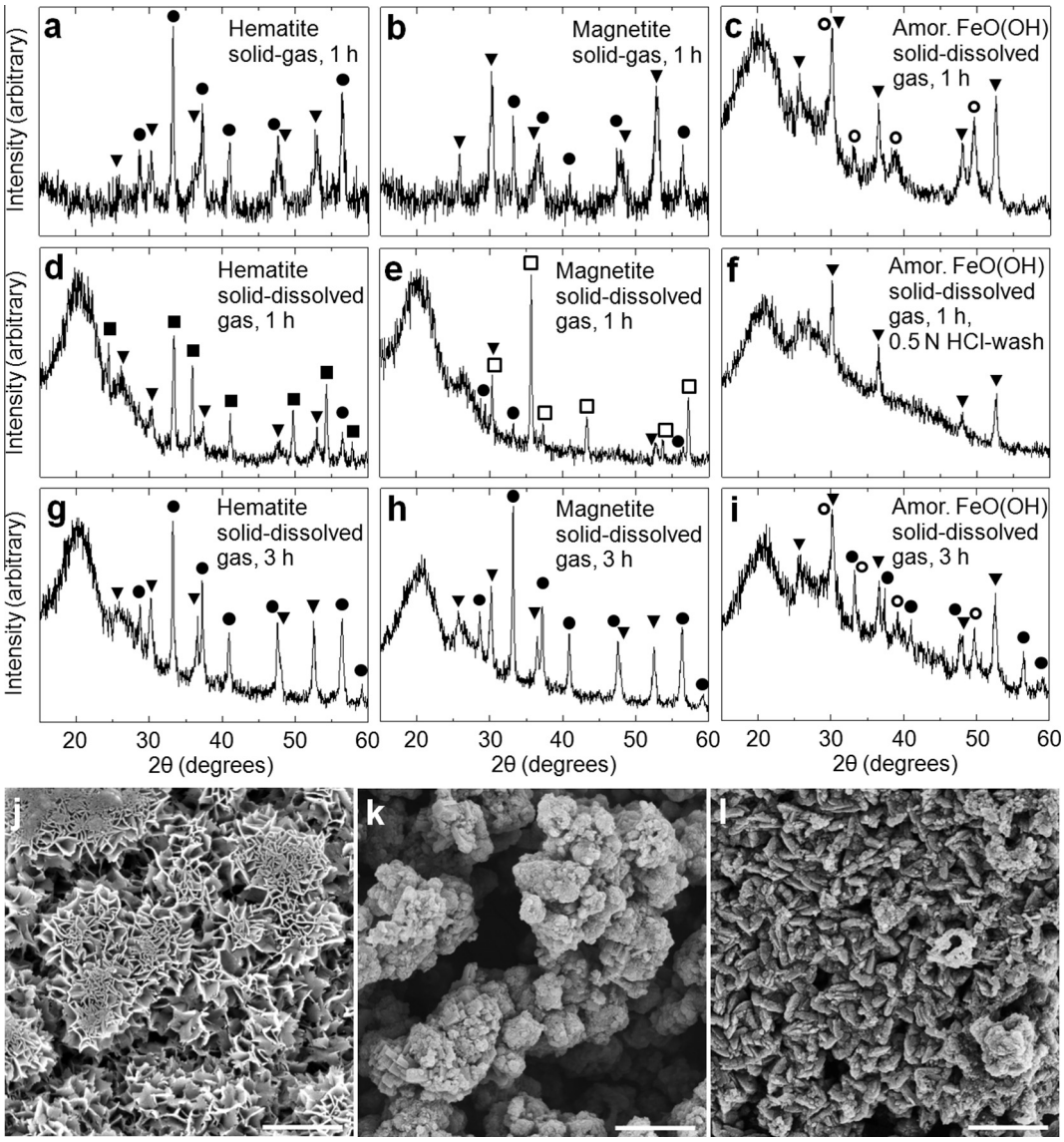

Fig. 4. Greigite preparations produced by solid–gas and solid–dissolved gas reactions. Hematite, magnetite, and amorphous FeO(OH) were subjected to solid–gas or solid–dissolved gas reactions for 1 h, unless otherwise indicated. Solid–dissolved gas reactions were also conducted for 3 h (g–i). The products were analyzed by XRD (a–i) and FE-SEM (j–l). Greigite preparations produced by solid–gas (a, j) and solid–dissolved gas (d, g) reactions with hematite, by solid–gas (b, k) and solid–dissolved gas (e, h) reactions with magnetite, and by solid–dissolved gas reaction with amorphous FeO(OH) (c, i) and the product from amorphous FeO(OH) after washing with 0.5 N HCl (f, l). Greigite, closed triangles. Hematite, closed squares. Mackinawite, open circles. Magnetite, open squares. Pyrite, closed circles. Bars: 1 μm.

prepared from hematite and magnetite, and of solid–dissolved gas reaction prepared from amorphous FeO(OH) followed by washing with 0.5 N HCl were individually tested by adding to Mc medium devoid of cysteine, a substrate of CDS involved in the biosynthesis of Fe–S clusters (Bandyopadhyay et al., 2008), although *M. jannaschii* was reported to have no CDS gene (Liu et al., 2010). Addition of either greigite preparation dramatically elevated stationary levels of methane concentration and the cell density to approximately 10- and 2-fold those in the absence of additives, respectively (Table 1). These results suggest that greigite promoted methanogenesis and growth, and the coexisting pyrite did not hinder the promotion. The concentration dependence indicated that sufficient enhancement of methanogenesis and growth occurred with 5 mg of the products from hematite (Table 1), and 1 mg was enough to promote methanogenesis to the level attained in the presence of 0.3% yeast extract (Fig. S2a).

The methanogenesis and growth effects might be related to the hydrogenotrophic nature and/or the S^0-reducing ability of *M. jannaschii* (Fig. 2). Therefore, other methanogens, including the hydrogenotrophic methanogen *Methanocaldococcus indicus* capable of reducing S^0 (L'Haridon et al., 2003), the hydrogenotrophic methanogen *Methanothermobacter thermautotrophicus* (Zeikus and Wolee, 1972) incapable of reducing S^0, and a heterotrophic

Table 1
Enhancement of methanogenesis and growth of *Methanocaldococcus jannaschii* by greigite.

Additive	Mineral composition	Methane (kPa)	Cell density ($\times 10^7$ cells/mL)
None	–	8 ± 1	3.1 ± 0.5
GPH	Greigite, Pyrite	77 ± 14	7.2 ± 0.4
1 mg		36 ± 6	5.1 ± 0.2
5 mg		85 ± 8	7.0 ± 0.6
10 mg		81 ± 4	6.7 ± 0.4
GPM	Greigite, Pyrite	60 ± 15	6.3 ± 0.5
G	Greigite	73 ± 13	6.2 ± 0.7

Notes: *M. jannaschii* was cultured in Mc medium lacking cysteine at 80 °C for 32 h. Greigite preparations were obtained by a 1-h solid–gas or solid–dissolved gas reaction with 0.63 mmol Fe source (hematite, magnetite, or amorphous FeO(OH)). The whole product or a designated amount of preparation from hematite was added to the culture. Solid–gas reactions and methanogen cultivation were performed in triplicate, and the results are shown as mean ± SD. GPH and GPM, products of solid–gas reactions of hematite (Fig. 4a) and magnetite (Fig. 4b), respectively. G, product of the solid–dissolved gas reaction of amorphous FeO(OH) followed by washing with 0.5 N HCl (Fig. 4f).

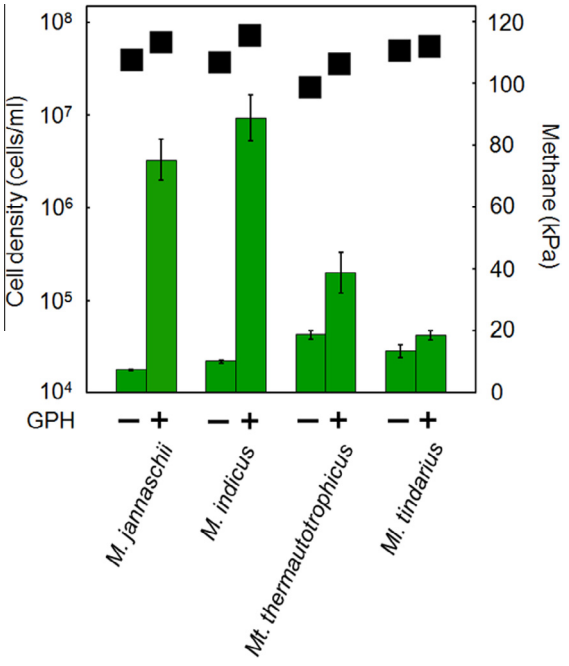

Fig. 5. Enhancement of methanogenesis and growth of methanogens by greigite. Methanogens were cultured in the absence or presence of greigite, and methane concentrations in the gas phase (green bars) and densities of free cells (plots) were measured. GPH, products of solid–gas reactions of hematite (Fig. 4a). The entire product obtained from a 1-h reaction (0.63 mmol Fe source) was added to the cultures. Mean ± SD ($n = 3$). (For interpretation of the references to colour in this figure legend, the reader is referred to the web version of this article.)

methanogen *Methanolobus tindarius* (König and Stetter, 1982) capable of reducing S^0 (Stetter and Gaag, 1983), were tested for any potential functional enhancement. Promotion of methanogenesis and growth was observed for *M. indicus* and *Mt. thermautotrophicus* but not for *Ml. tindarius* (Fig. 5), suggesting that the hydrogenotrophic nature, but not the S^0-reducing ability, may be related to these effects of greigite.

4. DISCUSSION

4.1. Comparison of solid–gas and solid–dissolved gas reactions

In this study, we developed abiotic solid–gas and solid–dissolved gas reactions of Fe(III)-oxide-hydroxides and H_2S, referring to the greigite synthesis by *M. jannaschii* from S^0 and hematite. The reactions appeared to depend essentially on the concentration and motility of H_2S. The higher reactivity observed in the solid–gas reactions than in the solid–dissolved gas reactions could be explained by the frequency of collisions between H_2S and Fe(III)-oxide-hydroxides, as both concentration and motility were higher in H_2S (g) than in H_2S (aq). Furthermore, the presence of charges at the structured water layer on the mineral surface in the solid–dissolved gas reaction may have interfered with the reactions involving H_2S (aq). During greigite synthesis in the solid–gas reactions, preservation of pre-existing Fe(III) under the completely anaerobic H_2S atmosphere must be essential, as Fe(II) oxidation under anaerobic conditions is essential for the polysulfide pathway.

4.2. Formulas of greigite/pyrite synthesis in solid–gas and solid–dissolved gas reactions

The conversion of hematite to amorphous FeS would be expressed as follows, assuming SO_2 as the oxidation product of H_2S; the other possible oxidation product, S^0, was never detected in the reaction.

$$Fe_2O_3 + 3H_2S \rightarrow 2FeS + H_2O + SO_2 + 2H_2 \quad (1)$$

Amorphous FeS was apparently transformed to greigite but amorphous FeS alone was not found to be a good substrate for greigite synthesis (Fig. S4f), indicating that both hematite and amorphous FeS were necessary to synthesize greigite.

$$Fe_2O_3 + FeS + 3H_2S \rightarrow Fe_3S_4 + 3H_2O \quad (2)$$

The greigite synthesis from hematite and H_2S is expressed by removing FeS from formulas (1) and (2).

$$3Fe_2O_3 + 9H_2S \rightarrow 2Fe_3S_4 + 7H_2O + SO_2 + 2H_2 \quad (3)$$

In contrast, greigite synthesis from magnetite could be explained by substituting S for O as an overall reaction via an intermediate.

$$Fe_3O_4 + 4H_2S \rightarrow Fe_3S_4 + 4H_2O \quad (4)$$

The difference in the reaction sequence could explain the difference in the morphologies between the hematite-derived flower-like structures and the magnetite-derived spherical structures of greigite/pyrite. Greigite synthesis from amorphous FeO(OH) would involve the formation of amorphous FeS from the reduction of amorphous FeO

(OH) with H_2S and the subsequent formation of greigite from amorphous FeO(OH), amorphous FeS, and H_2S. The total reaction would be expressed as follows.

$$6FeO(OH) + 10H_2S \rightarrow 2Fe_3S_4 + 8H_2O + 2SO_2 + 5H_2 \quad (5)$$

The mechanism of pyrite formation from greigite may not differ depending on the iron source for greigite synthesis; the S(–II) of H_2S and greigite would reduce the Fe(III) in greigite, as in the case of pyrite synthesis from amorphous FeS and H_2S (Drobner et al., 1990).

$$Fe_3S_4 + 2H_2S \rightarrow 3FeS_2 + 2H_2 \quad (6)$$

According to the above formulas, the syntheses of greigite/pyrite must produce stoichiometric amounts of H_2, which should be usable as the reductive force for production of organics (Heinen and Lauwers, 1996; Cody et al., 2000). In the solid–gas reactions of hematite and magnetite, however, H_2 production was over three orders of magnitude smaller than that of iron sources. Furthermore, the reaction of hematite was not inhibited by the bulk gas phase of H_2. These apparent discrepancies appear to be similar to that of pyrite synthesis (Drobner et al., 1990) and could be due to possible H_2-adsorbing properties of greigite (Cao et al., 2009) and/or pyrite. To test this hypothesis, liberation of H_2 from the minerals must be tested by applying voltage (Cao et al., 2009).

4.3. Stimulation of hydrogenotrophic methanogens by greigite

Greigite enhanced the methanogenesis and growth of hydrogenotrophic methanogens. Considering that these methanogens have membrane-bound hydrogenases harboring [4Fe–4S] clusters for the extraction of electrons from environmental H_2 (Thauer et al., 2010), we hypothesize that the Fe_4S_4 unit of greigite increased the amounts of these hydrogenases. The resulting increase in the hydrogenase activities may have contributed to the enhanced methanogenesis and growth. From a more speculative viewpoint, the Fe_4S_4 structure of greigite could be incorporated into the cells, considering that the methanogenesis and growth require proteins harboring different types of Fe–S clusters, which are known to be interconvertible even in vitro (Beinert et al., 1997). However, incorporation of a solid structure into a membrane component has not been demonstrated, and thus further research is required to clarify the mechanism of the enhancements. Liu et al. (2010) suggested that Fe–S clusters of archaea without CDS genes, such as *M. jannaschii*, are derived from inorganic sulfide. This study strongly suggests that greigite is one of these inorganic sulfides.

4.4. Biogenic greigite/pyrite

SRB are thought to be the only biological producer of pyrite in paleontology (Astafieva, 2005) because of their sulfide-producing nature. However, because the pH optima of most SRB are not lower than 6.5 (https://www.dsmz.de/catalogues/catalogue-microorganisms.html), their greigite/pyrite synthesis must be slower than that by *M. jannaschii*. Considering the pH dependence of greigite synthesis and that most *Methanocaldococcus* species reported to date are suggested to grow well at pH 6.0 (http://jcm.brc.riken.jp/ja/catalogue), the possible involvement of *Methanocaldococcus* species in biological greigite/pyrite production cannot be ignored. Nevertheless, the predominance of SRB in biological greigite/pyrite synthesis seems to stand at non-hyperthermophilic temperatures, since most non-hyperthermophilic methanogens have pH optima in the range similar to that of SRB (https://www.dsmz.de/catalogues/catalogue-microorganisms.html) and thus are not expected to be involved in greigite synthesis, even if they can reduce S^0.

4.5. Greigite synthesis in the Hadean Eon

Even in the anaerobic Hadean Eon, hematite was present (Hazen, 2013), and magnetite and amorphous FeO(OH) were routinely produced by the serpentinization of olivine (Janecky and Seyfried, 1986) and UV oxidation of oceanic surface Fe(II) (Braterman et al., 1983), respectively. These Fe(III)-oxide-hydroxides must have reacted with H_2S (aq) emitted from acidic hydrothermal vents in the acidulous ocean (Macleod et al., 1994; Russell and Hall, 2006) to produce greigite. Greigite synthesis may have been more ubiquitous than was expected from the polysulfide pathway, given that the polysulfide pathway occurs only at alkaline hydrothermal vents, which are quite rare compared to acidic hydrothermal vents (Kelley et al., 2001). Greigite synthesis by the solid–gas reactions may have astrobiological significance. Fe–S clusters are necessarily present in organisms on Earth, and possibly in organisms on other planets. If greigite is the origin of Fe–S clusters, as postulated by Russell and Martin (2004) and supported by data from the present study, then the presence of greigite would be a prerequisite for the development of similar life forms. Results from the present study suggested that the presence of a combination of Fe(III)-oxide-hydroxides and H_2S is sufficient to predict the occurrence of greigite.

5. CONCLUSIONS

The hyperthermophilic hydrogenotrophic methanogen *M. jannaschii* was found to be able to reduce S^0. The resulting H_2S (aq) produced amorphous FeS, greigite, and pyrite from extracellular hematite. Inspired by the greigite synthesis by *M. jannaschii*, we established conditions for abiotic reactions of hematite with H_2S for greigite formation. Greigite formed faster with H_2S (g) than with H_2S (aq), indicating that sulfide ions may not be involved in greigite formation. Magnetite and amorphous FeO(OH) were also converted to greigite by reactions with H_2S (g) and H_2S (aq). The Fe(III) present in oxides and hydroxides, which was preserved under H_2S-derived completely anaerobic conditions, is likely essential for greigite synthesis. The solid–gas reaction of hematite and H_2S (g) occurred without preference for a pre-existing anaerobic gas phase and at temperatures as low as 40 °C. From a practical aspect, the solid–dissolved gas reactions appeared to represent greigite synthesis in nature. The obtained greigite enhanced

methanogenesis and growth of hydrogenotrophic methanogens, i.e., it was bioactive. This finding reinforces the perspective that greigite is the origin of the [4Fe–4S] cluster.

FUNDING

This study was supported by the Japan Society for the Promotion of Science KAKENHI Grant Number 26420881 to T.K. and by a Sasakawa Scientific Research Grant from The Japan Science Society, Grant Number 25-637, to K.I. The funding sources had no role in study design; in the collection, analysis, and interpretation of data; in the writing of the report; or in the decision to submit the article for publication.

CONFLICTS OF INTEREST

The authors have no conflicts of interest to declare.

ACKNOWLEDGEMENTS

We thank T. Adachi for technical help with XRD analysis. We also thank Editage (www.editage.jp) for English language editing.

APPENDIX A. SUPPLEMENTARY DATA

Supplementary data associated with this article can be found, in the online version, at http://dx.doi.org/10.1016/j.gca.2016.07.005.

REFERENCES

Apostolova R. D., Kolomoets O. V. and Shembel' E. M. (2009) Electrolytic iron sulfides for thin-layer lithium-ion batteries. *Russ. J. Appl. Chem.* **82**, 1939–1943.

Astafieva M. M. (2005) Nature of framboidal structures in black shales (the Cambrian of the Siberian platform and the Permian of the Barents sea shelf). In *Perspectives in Astrobiology* (eds. R. B. Hoover, A. Y. Rozanov and R. R. Paepe). IOS Press, Amsterdam, pp. 1–5.

Bandyopadhyay S., Chandramouli K. and Johnson M. K. (2008) Iron-sulphur cluster biosynthesis. *Biochem. Soc. Trans.* **36**, 1112–1119.

Bauer E., Man K. L., Pavlovska A., Locatelli A., Menteş T. O., Niño M. A. and Altman M. S. (2014) Fe_3S_4 (greigite) formation by vapor-solid reaction. *J. Mater. Chem. A* **2**, 1903–1913.

Beinert H., Holm R. H. and Münck E. (1997) Iron-sulfur clusters: nature's modular, multipurpose structures. *Science* **277**, 653–659.

Berner R. A. (1964) Iron sulfides formed from aqueous solution at low temperatures and atmospheric pressure. *J. Geol.* **72**, 293–306.

Berner R. A. (1984) Sedimentary pyrite formation: an update. *Geochim. Cosmochim. Acta* **48**, 605–615.

Bertel D., Peck J., Quick T. J. and Senko J. M. (2012) Iron transformations induced by an acid-tolerant *Desulfosporosinus* species. *Appl. Environ. Microbiol.* **78**, 81–88.

Braterman P. S., Cairns-Smith A. G. and Sloper R. W. (1983) Photo-oxidation of hydrated Fe^{2+}-significance for banded iron formations. *Nature* **303**, 163–164.

Brock T. D. and Od'ea K. (1977) Amorphous ferrous sulfide as a reducing agent for culture of anaerobes. *Appl. Environ. Microbiol.* **33**, 254–256.

Butler I. B. and Rickard D. (2000) Framboidal pyrite formation via the oxidation of iron (II) monosulfide by hydrogen sulphide. *Geochim. Cosmochim. Acta* **64**, 2665–2672.

Cao F., Hu W., Zhou L., Shi W., Song S., Lei Y., Wang S. and Zhang H. (2009) 3D Fe_3S_4 flower-like microspheres: high-yield synthesis via a biomolecule-assisted solution approach, their electrical, magnetic and electrochemical hydrogen storage properties. *Dalton Trans.*, 9246–9252.

Cenens J. and Schoonheydt R. A. (1988) Visible spectroscopy of methylene blue on hectorite, laponite B, and barasym in aqueous suspension. *Clay. Clay Miner.* **36**, 214–224.

Chang Y.-S., Savitha S., Sadhasivam S., Hsu C.-K. and Lin F.-H. (2011) Fabrication, characterization, and application of greigite nanoparticles for cancer hyperthermia. *J. Colloid Interface Sci.* **363**, 314–319.

Chen J.-S. and Mortenson L. E. (1977) Inhibition of methylene blue formation during determination of the acid-labile sulfide of iron-sulfur protein samples containing dithionite. *Anal. Biochem.* **79**, 157–165.

Chen X., Zhang X., Wan J., Wang Z. and Qian Y. (2005) Selective fabrication of metastable greigite (Fe_3S_4) nanocrystallites and its magnetic properties through a simple solution-based route. *Chem. Phys. Lett.* **403**, 396–399.

Cody G. D., Boctor N. Z., Filley T. R., Hazen R. M., Scott J. H., Sharma A. and Yoder H. S. (2000) Primordial carbonylated iron-sulfur compounds and the synthesis of pyruvate. *Science* **289**, 1337–1340.

Cornwell J. C. and Morse J. W. (1987) The characterization of iron sulfide minerals in anoxic marine sediments. *Marine Chem.* **22**, 193–206.

Dekkers M. J. and Schoonen M. A. A. (1994) An electrokinetic study of synthetic greigite and pyrrhotite. *Geochim. Cosmochim. Acta* **58**, 4147–4153.

Drobner E., Huber H., Wächtershäuser G., Rose D. and Stetter K. O. (1990) Pyrite formation linked with hydrogen evolution under anaerobic conditions. *Nature* **346**, 742–744.

Feng M., Lu Y., Yang Y., Zhang M., Xu Y.-J., Gao H.-L., Dong L., Xu W.-P. and Yu S.-H. (2013) Bioinspired greigite magnetic nanocrystals: chemical synthesis and biomedicine applications. *Sci. Rep.* **3**, 1–6.

Hazen R. M. (2013) Paleomineralogy of the Hadean eon: a preliminary species list. *Am. J. Sci.* **313**, 807–843.

Heinen W. and Lauwers A. M. (1996) Organic sulfur compounds resulting from the interaction of iron sulfide, hydrogen sulfide and carbon dioxide in an anaerobic aqueous environment. *Origins Life Evol. Biosphere* **26**, 131–150.

Hunger S. and Benning L. G. (2007) Greigite: a true intermediate on the polysulfide pathway to pyrite. *Geochem. Trans.* **8**, 1.

Igarashi K. and Kuwabara T. (2014) Fe(III) oxides protect fermenter-methanogen syntrophy against interruption by elemental sulfur via stiffening of Fe(II) sulfides produced by sulfur respiration. *Extremophiles* **18**, 351–361.

Janecky D. R. and Seyfried, Jr., W. E. (1986) Hydrothermal serpentinization of peridotite within the oceanic crust: Experimental investigations of mineralogy and major element chemistry. *Geochim. Cosmochim. Acta* **50**, 1357–1378.

Jones W. J., Leigh J. A., Mayer F., Woese C. R. and Wolfe R. S. (1983) *Methanococcus jannaschii* sp. nov., an extremely thermophilic methanogen from a submarine hydrothermal vent. *Arch. Microbiol.* **136**, 254–261.

Kajander E. O., Ciftcioglu N., Aho K. and Garcia-Cuerpo E. (2003) Characteristics of nanobacteria and their possible role in stone formation. *Urol. Res.* **31**, 47–54.

Kelley D. S., Karson J. A., Blackman D. K., Fruh-Green G. L., Butterfield D. A., Lilley M. D., Olson E. J., Schrenk M. O., Roe K. K., Lebon G. T., Rivizzigno P. and Party A.-S. (2001) An off-axis hydrothermal vent field near the Mid-Atlantic Ridge at 30° N. *Nature* **412**, 145–149.

König H. and Stetter K. O. (1982) Isolation and characterization of *Methanolobus tindarius*, sp. nov., a coccoid methanogen growing only on methanol and methylamines. *Zbl. Bakt. Hyg. I. Abt. Orig. C* **3**, 478–490.

Kuwabara T. and Igarashi K. (2012) Microscopic studies on *Thermosipho globiformans* implicate a role of the large periplasm of Thermotogales. *Extremophiles* **16**, 863–870.

Lefèvre C. T., Menguy N., Abreu F., Lins U., Pósfai M., Prozorov T., Pignol D., Frankel R. B. and Bazylinski D. A. (2011) A cultured greigite-producing magnetotactic bacterium in a novel group of sulfate-reducing bacteria. *Science* **334**, 1720–1723.

L'Haridon S., Reysenbach A.-L., Banta A., Messner P., Schumann P., Stackebrandt E. and Jeanthon C. (2003) *Methanocaldococcus indicus* sp. nov., a novel hyperthermophilic methanogen isolated from the Central Indian Ridge. *Int. J. Syst. Evol. Microbiol.* **53**, 1931–1935.

Liu Y., Sieprawska-Lupa M., Whitman W. B. and White R. H. (2010) Cysteine is not the sulfur source for iron-sulfur cluster and methionine biosynthesis in the methanogenic archaeon *Methanococcus maripaludis*. *J. Biol. Chem.* **285**, 31923–31929.

Lovley D. R. and Phillips E. J. P. (1986) Organic matter mineralization with reduction of ferric iron in anaerobic sediments. *Appl. Environ. Microbiol.* **51**, 683–689.

Macleod G., McKeown C., Hall A. J. and Russell M. J. (1994) Hydrothermal and oceanic pH conditions of possible relevance to the origin of life. *Orig. Life Evol. Biosphere* **24**, 19–41.

Mountfort D. O. and Asher R. A. (1979) Effect of inorganic sulfide on the growth and metabolism of *Methanosarcina barkeri* strain DM. *Appl. Environ. Microbiol.* **37**, 670–675.

Paolella A., George C., Povia M., Zhang Y., Krahne R., Gich M., Genovese A., Falqui A., Longobardi M., Guardia P., Pellegrino T. and Manna L. (2011) Charge transport and electrochemical properties of colloidal greigite (Fe_3S_4) nanoplatelets. *Chem. Mater.* **23**, 3762–3768.

Rickard D. and Luther, III, G. W. (2007) Chemistry of iron sulfides. *Chem. Rev.* **107**, 514–562.

Roldan A., Hollingsworth N., Roffey A., Islam H.-U., Goodall J. B. M., Catlow C. R. A., Darr J. A., Bras W., Sankar G., Holt K. B., Hogarth G. and de Leeuw N. H. (2015) Bio-inspired CO_2 conversion by iron sulfide catalysts under sustainable conditions. *Chem. Commun.* **51**, 7501–7504.

Russell M. J. and Hall A. J. (1997) The emergence of life from iron monosulphide bubbles at a submarine hydrothermal redox and pH front. *J. Geol. Soc. London* **154**, 377–402.

Russell M. J. and Hall A. J. (2006) The onset and early evolution of life. *Geol. Soc. Am.* **198**, 1–32.

Russell M. J. and Martin W. (2004) The rocky roots of the acetyl-CoA pathway. *Trends Biochem. Sci.* **29**, 358–363.

Skinner B. J., Erd R. C. and Grimaldi F. S. (1964) Greigite, the thio-spinel of iron; a new mineral. *Am. Mineralogist* **49**, 543–555.

Snoeyink V. L. and Jenkins D. (1980) *Water Chemistry*. John Wiley & Sons, New York.

Sørensen J. (1982) Reduction of ferric iron in anaerobic, marine sediment and interaction with reduction of nitrate and sulfate. *Appl. Environ. Microbiol.* **43**, 319–324.

Stetter K. O. and Gaag G. (1983) Reduction of molecular sulphur by methanogenic bacteria. *Nature* **305**, 309–311.

Stookey L. L. (1970) Ferrozine–a new spectrophotometric reagent for iron. *Anal. Chem.* **42**, 779–781.

Thauer R. K., Kaster A.-K., Goenrich M., Schick M., Hiromoto T. and Shima S. (2010) Hydrogenases from methanogenic archaea, nickel, a novel cofactor, and H_2 storage. *Annu. Rev. Biochem.* **79**, 507–536.

Wächtershäuser G. (1992) Groundworks for an evolutionary biochemistry: the iron-sulphur world. *Prog. Biophys. Mol. Biol.* **58**, 85–201.

Wada H. (1977) The synthesis of greigite from a polysulfide solution at about 100 °C. *Bull. Chem. Soc. Jpn.* **50**, 2615–2617.

Zeikus J. G. and Wolee R. S. (1972) *Methanobacterium thermoautotrophicus* sp. n., an anaerobic, autotrophic, extreme thermophile. *J. Bacteriol.* **109**, 707–713.

Associate editor: Thomas McCollom